Jurnal Teknologi

Full paper

CMOS-MEMS Integration in Micro Fabry Perot Pressure Sensor Fabrication

Nor Hafizah Ngajikin[a*], Low Yee Ling[a], Nur Izzati Ismail[a], Abu Sahmah Mohd Supaát[a], Mohd Haniff Ibrahim[a], Norazan Mohd Kassim[a]

[a]*Lightwave Communication Research Group, Fakulti Kejuruteraan Elektrik, Universiti Teknologi Malaysia, 81310 UTM Johor Bahru, Johor*

*Corresponding author: nhafizah@fke.utm.my

Article history

Received :12 July 2012
Received in revised form :
4 April 2013
Accepted :15 April 2013

Graphical abstract

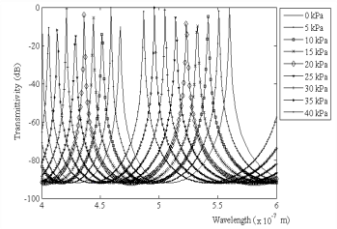

Abstract

Integration of Complimentary Metal-Oxide-Semiconductor (CMOS) and Microelectromechanical System (MEMS) technology in Fabry Perot blood pressure sensor (FPPS) fabrication processes is presented. The sensor that comprises of a 125 µm diameter of circular diaphragm is modeled to be fabricated using integration of CMOS-MEMS technology. To improve the sensor reliability, a sleeve structure is designed at the back of Silicon wafer by using MEMS Deep Reactive ion Etching (DRIE) process for fiber insertion, which offers a large bonding area. Optical light source at 550 nm wavelength is chosen for this device. The sensor diaphragm mechanic deflection and its optical spectrum is theoretically analyzed and simulated. The analytical results show high linear response in the range of 0 to 40 kPa and a reasonable sensitivity of 1.83 nm/kPa (spectrum shift/pressure) has been obtained for this sensor. The proposed integration of CMOS-MEMS technology limit the material selection yet produces an economical method of FPPS fabrication and integrated system.

Keywords: Fabry Perot pressure sensor; CMOS; MEMS; internal blood pressure

Abstrak

Integrasi teknologi *Complimentary Metal-Oxide-Semiconductor* (CMOS) dan *Microelectromechanical System* (MEMS) dalam fabrikasi pengesan tekanan darah *Fabry Perot* (FPPS) dibentangkan dalam artikel ini. Pengesan dengan 125 µm diameter bulatan membran dimodelkan untuk fabrikasi menggunakan teknologi ini. Bagi meningkatkan keboleh-harapan pengesan, struktur lengan telah direkabentuk di bahagian belakang wafer Silicon menggunakan proses MEMS *Deep Reactive ion Etching* (DRIE) untuk masukan fiber optik dengan lebih permukaan melekat. Sumber cahaya pada jalur gelombang tengah 550 nm dipilih untuk pengesan ini. Lengkok mekanik dan spectrum optic bagi pengesan ini dianalisis dan simulasi secara teoritikal. Keputusan analitikal menunjukkan hubungan linar bagi 0 hingga 40 kPa tekanan darah dengan ketelitian sebanyak 1.83 nm/kPa (pindahan spectrum/tekanan) telah diperolehi. Cadangan gabungan teknologi CMOS dan MEMS ini mengehadkan pilihan bahan, namun telah menghasilkan kaedah fabrikasi yang ekonomi serta peluang untuk integrasi dengan sistem lain.

Kata kunci: Pengesan tekanan Fabry Perot; CMOS; MEMS; tekanan darah

1.0 INTRODUCTION

Human blood pressure can be measured either using direct or indirect method depending on its data accuracy requirement. Indirect blood pressure measurement is conducted at outer of human body where a device named as sphygmomanometer is used to read the blood pressure. This indirect method however produces data with less accuracy compared to a direct measurement method. In direct blood pressure measurement, the data is more accurate since it involves a sensor that is in-contact with human blood vessel.[1] This type of measurement produces high accuracy of blood pressure data that are needed during medical surgical operation. This procedure will ensure that patient blood pressure is maintained at a normal level. Since the sensor is located in blood vessel, the configuration of blood pressure sensor must be smaller than the blood vessel. The need for the small size sensor attracts invention in fiber optic sensor for biomedical application.[2-3] Micro optical Fabry-Perot pressure sensor (FPPS) is one of the optical sensors that has a huge potential in providing accurate, robust and reliable sensor in medical field.[3-8]

In the literature, FPPS have been fabricated using Micro-electro-mechanical System (MEMS) technology. [3-8] Merits of the MEMS technology is proved in manufacturing sensor diaphragm with small size and variation of material selection. This technology, however consumes high fabrication cost. In MEMS fabrication, configuration and material used for MEMS device design is very

broad thus require a variety of process standard and machines. In contrast, CMOS technology has clearly stated the material and configuration in its standards. These standards lead to a development of several CMOS foundry that offers fabrication with similar specifications and machines. This is the reason why integration of CMOS with MEMS technology reduces the cost of FPPS fabrication. This proposed fabrication not only offers an economical method in fabricating MEMS device yet provides platform for integration with other electronic devices.

In this paper, we report and demonstrate for the first time, to the best of our knowledge, an integration of CMOS-MEMS technology, cost-effective way in fabricating micro FPPS for blood pressure sensor application. The proposed sensor is designed for aortic-pressure waveform monitoring application with pressure measurement range from 0 to 40 kPa. The FPPS has been modeled to be fabricated using CMOS-MEMS fabrication. This method split the fabrication processes into two phases; CMOS and MEMS. CMOS fabrication process is modeled to form FPPS sensor diaphragm with pool structure for sensor sensitivity enhancement while the MEMS process is modeled after the CMOS fabrication for FPPS mirror, FPPS cavity and sleeve structure for fiber insertion.

■2.0 FPPS DESIGN

2.1 FPPS Working Principle

In general, FPPS consists of a Fabry Perot (FP) cavity attached to an optical fiber tip. Figure 1 illustrates the configuration of the proposed FPPS. Two parallel mirrors separated by a FP cavity, *d* form a FP interferometer. To work as a pressure sensor, the outer mirror that holds by a diaphragm must be movable so it can sense the pressure variation. Key of the FPPS operation lay on the relationship between length of FP cavity, *d* and the output spectrum. Velocity of blood in human artery produces a uniform pressure that will cause diaphragm deflection followed by a change in *d*. In FP interferometer, different value of *d* will produce different value of operating wavelength, λ. Therefore, different blood pressure can be detected by measuring the wavelength spectrum shift. Operating wavelength, λ for a specific length of cavity can be found by solving equation (1).[12]

$$\lambda = \frac{2n_2 d}{m}\sqrt{1-\left(\frac{\sin\theta}{n_2}\right)^2} \quad (1)$$

where *m* is mode number inside the cavity, n_2 is material refractive index inside the cavity and θ is light incident angle. In this paper, the light incident angle is assumed to be 0^o and the refractive index of FP cavity is 1.0.

In this paper, the sleeve structure is adopted from Li M. *et al.*[6] while pool on the top of the diaphragm is adopted from Xiao Q. N. *et al.*[7]. As shown in Figure 1, the right side of this structure consists of a Silicon (Si) diaphragm attached with an Aluminum (Al) mirror. The other mirror is deposited at the tip of optical fiber. A sleeve-type structure with 125µm diameter at the other side of Si wafer forms a FP cavity and sensor-fiber locking mechanism. The pool type structure on top of sensor diaphragm has been experimentally proved to enhance the sensor sensitivity.[7] However, the pool parameters that influence the sensor performance are not analyzed in this paper.

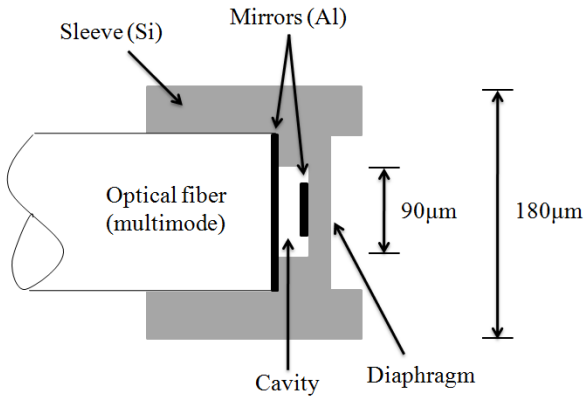

Figure 1 Proposed structure of sleeve-type FPPS

2.2 FPPS Diaphragm Design

FPPS diaphragm is a crucial part in this device since it will determine the sensor sensitivity and accuracy. In literature, material with small value of Young's modulus will enhance the sensitivity of MEMS FPPS. Some of the MEMS pressure sensor diaphragm have been designed and fabricated using polymeric material.[5,11] In this paper, Si film is chosen due to a restriction of material in CMOS fabrication standard. Although Si has higher of Young's modulus compared to polymeric material, it has been proven to work well in literature.[6-7] Furthermore, the Si diaphragm offers good linearity with applied pressure.

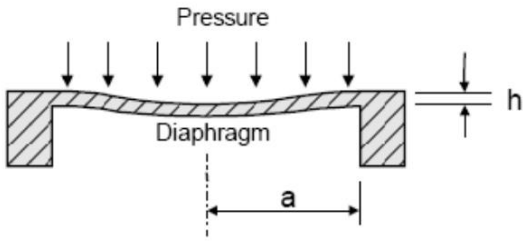

Figure 2 Structure of a circular diaphragm

The proposed FPPS diaphragm is in a circular shape as shown in Figure 2. Assuming a uniform pressure, *P* applied on the diaphragm surface, there will be a maximum deflection at the center of diaphragm structure. For this structure, the maximum central deflection, ω_c due to a loaded pressure, *P* and fixed radius, *a* is given by [6]

$$\omega_c = \frac{3Pa^4(1-v^2)}{16Eh^3} \quad (2)$$

where E is Young's modulus of diaphragm material, v is the Poisson's ratio of diaphragm material and h is the thickness of the sensor diaphragm. The diaphragm thickness is designed such that the deflection is less than $1/3$ of the initial length of cavity at maximum pressure. The 1/3 of FP length of cavity value is an analytical breakpoint for diaphragm mechanic deflection.[14] Based on equation (2) the FPPS diaphragm configurations are listed in Table 1.

Table 1 Parameters of FPPS silicon diaphragm

Radius of diaphragm, a	Diaphragm thickness, h	Young's modulus, E	Poisson ratio, v	Applied Pressure, P
45 µm	1 µm	160 GPa	0.22	0 - 40 kPa

3.0 FPPS CMOS-MEMS FABRICATION PROCESS

The integration of CMOS-MEMS can be accomplished in three different ways. The steps can be added on either before the standard CMOS process sequence (pre-CMOS), in between regular CMOS process (intra-CMOS) or after completion of CMOS process (post-CMOS). As afore mentioned, the proposed FPPS is modeled to be fabricated using post-CMOS process. To fabricate MEMS device using integration of CMOS-MEMS process, the materials are limited to the material in CMOS foundry. In this paper, the CMOS technology is based on SilTerra 0.18 µm standard.[15]

Figure 3 shows cross-sectional view and mask layout of the proposed FPPS structure. Top region of this cross-section is modeled to be fabricated using CMOS technology while the bottom region is modeled to be fabricated using MEMS technology. In this paper, positive polarity of photoresist is selected for the patterning process. Only 3 masks are needed for the whole fabrication process. A multi-mode fiber with 62.5/125µm (core/cladding diameter) is used in this sensor system. Therefore, an exact circular sleeve-type structure with 125µm diameter is etched at the backside of Si wafer for locking mechanism. In this proposed fabrication model, 1µm thickness of Aluminum (Al) thin film that function as FP mirror is evaporated at the bottom side of Si diaphragm and another mirror at the tip of optical fiber. 1.4 µm air gap between these two Al films form a FP cavity. Details of the CMOS-MEMS fabrication process step are discussed in the following section.

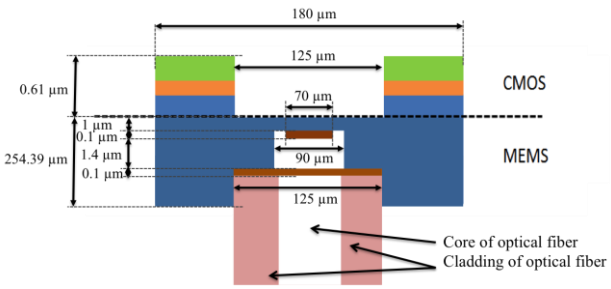

(a) Cross-sectional view

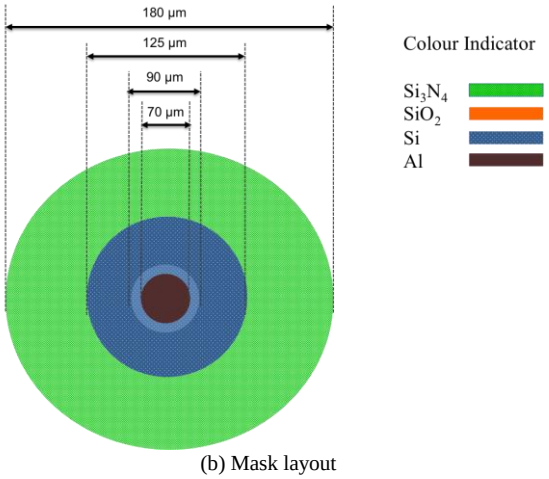

(b) Mask layout

Figure 3 Cross-sectional view and mask layout of CMOS-MEMS FPPS

3.1 FPPS Fabrication Model

In this section, fabrication process model for each technology, CMOS and MEMS are discussed in detail.

3.1.1 CMOS Process Sequence in FPPS Fabrication

The CMOS fabrication process steps for the proposed FPPS fabrication are based on SilTerra 0.18 µm technology. Therefore, all the process details and material must comply with the standard. In this sub-section, a model of CMOS fabrication process is presented to form a FPPS pool structure. 255 µm thickness and 4 inch diameter of Si wafer is used in this fabrication model.

Figure 4 describes the graphical cross-sectional view of the CMOS FPPS process step. In this CMOS technology, the pool on top of Si diaphragm is formed by 0.01 µm thickness of SiO_2 and 0.1 µm thickness of Si_3N_4 film. The SiO_2 film is modeled to be developed using thermal oxidation process while Si_3N_4 film is modeled to be deposited using low-pressure chemical vapor deposition (LPCVD) process. To shape the pool structure, both films are modeled to be etched using reactive ion etching (RIE) process. To increase the pool depth, 0.5 µm deep of RIE process on topside of Si wafer is modeled. In literature, the pool structure improves the sensor sensitivity by increasing the blood pressure on the sensor diaphragm.[6-7] The sensitivity improvement due to this structure, however, is not discussed in this paper.

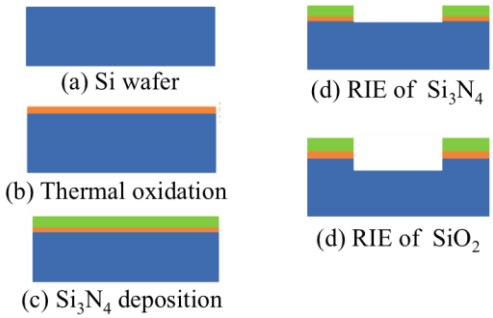

Figure 4 CMOS process step for FPPS fabrication

3.1.2 MEMS Processes

MEMS technology is used to model the fabrication of FP mirror, sensor diaphragm and sleeve structure of FPPS. Process step and the wafer cross-section are illustrated in Figure 5. In this model, 2 stage of deep reactive ion etch (DRIE) are modeled to be fabricated on the backside of the Si wafer. The first DRIE process is model to be done for a targeted 253.7 µm depth. This process will form a sleeve structure for fiber insertion and locking mechanism for the sensor. The second DRIE process will create 1.5 µm deep of circular shape cavity on the center of FPPS backside structure. These two DRIE processes will form 1 µm thickness of Si sensor diaphragm. Then, 0.1 µm thickness of Al film is modeled to be evaporated on the backside of this wafer and at the tip of optical fiber to form a FP mirror. The fiber then needs to be inserted on the backside of Si wafer to complete the sensor fabrication process as visualized in Figure 3.

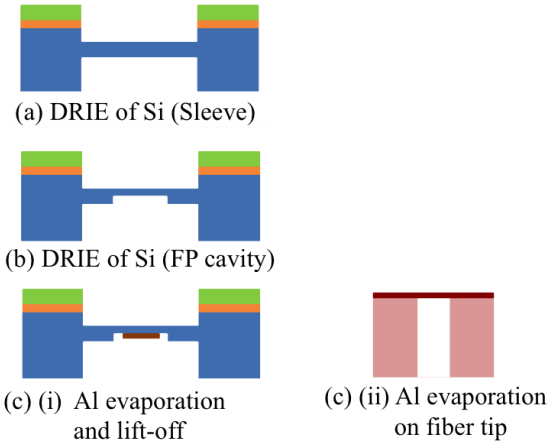

Figure 5 MEMS process steps for FPPS fabrication

■4.0 FPPS PERFORMANCE ANALYSIS

In this section, the relationship between internal blood pressure mechanic diaphragm deflection and optical performance are discussed.

4.1 Diaphragm Deflection Analysis

Theoretical analysis on equation 2 produces a relationship between diaphragm deflections for 0 to 40 kPa of internal blood pressure. Based on material properties listed in Table 1, analysis on the sensor diaphragm deflection is done using Matlab® mathematical software and presented in Figure 6. The Si diaphragm produces a linear deflection for a given pressure. In blood pressure sensor application, linearity of the deflection enhances the accuracy of data analysis. In this analysis, it shows that Si material as a diaphragm produces good linearity for the proposed sensor structure. Maximum internal blood pressure, 40 kPa is calculated to generate 182.9 nm deflection in which change the length of FP cavity to 1217.1 nm. This 182.9 nm deflection is 39% from the diaphragm breakpoint. This value indicates reliability of the sensor diaphragm.

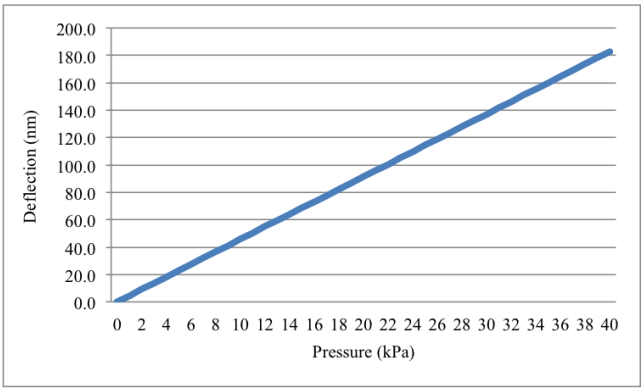

Figure 6 Linear relationship between FPPS diaphragm deflection with internal blood pressure

4.1 Optical Analysis

As mentioned previously, mechanic deflection of the proposed sensor diaphragm varies the length of FP cavity. In Figure 6, it is shown that 0 to 40 kPa of internal blood pressure exhibit 0 to 182.9 nm diaphragm deflection. In optical analysis, this deflection will produce 1217.1 nm to 1400 nm range of length of cavity, *d*. Operating wavelength for selected pressure is plotted in Figure 7. For 0 to 40 kPa internal blood pressure, the sensor operates at 486.8 nm to 560 nm wavelength range. Figure 7 shows that free spectral range (FSR) for the designed 0 to 40 kPa internal blood pressure FPPS have no overlapping between operating and its auxiliary wavelength.

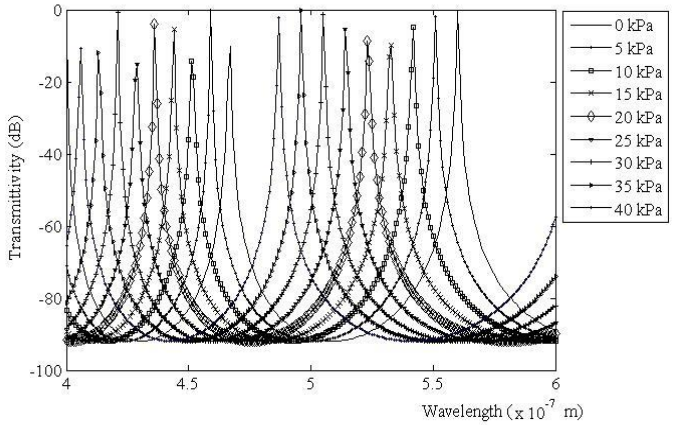

Figure 7 Relationship between pressures with optical wavelength

■5.0 CONCLUSION

Micro optical Fabry-Perot pressure sensor fabrication using integration of CMOS-MEMS technology has been modeled in this paper. CMOS technology has been modeled to form the diaphragm pool for sensitivity enhancement while MEMS technology is employed for FP cavity, FP mirror and sleeve-type structure fabrication. Analysis of 1 µm thickness of Si diaphragm deflection shows good linearity with the applied pressure. Theoretical analysis also shows that 0 to 182.9 nm sensor diaphragm deflection shifts the optical operating wavelength from 560 nm to 486.8 nm wavelength respectively. In the aspect of fabrication, this paper has modeled the fabrication in ideal case. In practical, parameter involve in each fabrication recipe to be critically analyze in order to produce a perfect configuration of FPPS.

Acknowledgement

Authors would like to thanks Universiti Teknologi Malaysia for providing research grant (4P015) for this research work.

References

[1] Dorf, R. C. 2006. *The Electrical Engineering Handbook: Sensors, Nanoscience, Biomedical Engineering, and Instruments*. CRC/Taylor & Francis.
[2] Polanyi M. 1965. *Medical applications of Fiber Optics*. In *Conference Medical Electronic Biology Engineering*. Tokyo. 598–599.
[3] Shimada, M. *et al*. 2009. Ultra-miniature Optical Fiber Pressure Sensor with a Sleeve for Catheter Insertion. *Electronics and Communications in Japan*. 92(8): 36–42.

[4] Shimada, M., Y. Kinefuchi, and K. Takahashi. 2008. Sleeve-Type Ultra Miniature Optical Fiber Pressure Sensor Fabricated by DRIE. *Sensors Journal IEEE*. 8(7): 1337–1341.
[5] Melamud, R., *et al.* 2007. SU-8 MEMS Fabry-Perot Pressure Sensor. *Sensors and Actuators A. Physical.* 138(1): 52–62.
[6] Li, M., M. Wang, and H. Li. 2006. Optical MEMS Pressure Sensor Based on Fabry-Perot Interferometry. *Opt. Express*. 14(4): 1497–1504.
[7] Xiao Q. N., *et al*. 2006. An Optical Fibre MEMS Pressure Sensor using Dual-Wavelength Interrogation. Institute of Physics (IOP) Publishing. *Journal of Measurement and Science Technology*. 17: 2401–2404.
[8] Watson Stuart, G. M. J., and Jones. Julian D. C. 2006. Laser-machined Fibes as Fabry-Perot Pressure Sensors. *Applied Optics*. 45: 5590–5596.
[9] Saran, A., D. C. Abeysinghe, and J. T. Boyd. 2006. Microelectromechanical System Pressure Sensor Integrated Onto Optical Fiber by Anodic Bonding. *Appl. Opt*. 45(8): 1737–1742.
[10] Chen, F. U. *et al.* 2005. CMOS-MEMS Resonant RF Mixer-filters, Micro Electro Mechanical Systems. MEMS2005. 18th IEEE International Conference on 30 Jan.-3 Feb. 24–27
[11] Cibula, E.a.D.D. 2005. Miniature Fiber-optic Pressure Sensor with a Polymer Diaphragm. *Appl. Opt*. 44(4): 2736–2744.
[12] Tucker R. S., *et al*. 2002. Thermal Noise and Radiation Pressure in MEMs Fabry Perot Tunable Filters and Lasers. *IEEE Journal on Selected Topics on Quantum Electronics*. 8(1).
[13] Hsu, T. R. 2008. *Mems and Microsystems: Design, Manufacture, and Nanoscale Engineering*. John Wiley. 550.
[14] Ngajikin N. H. *et al*. 2011. MEMS Fabry Perot Optical Tuning Filter: Modeling an Electrostatic and Mechanic Beam Deflection. *Microsystem Technologies*. Springer. 17(1): 19–25.
[15] Baltes, H. *et al.* 2008. *CMOS-MEMS: Advanced Micro and Nanosystems*. John Wiley & Sons.